Acta Cryst E CRYSTALLOGRAPHIC COMMUNICATIONS

ISSN 2056-9890

Synthesis, crystal structure and Hirshfeld surface analysis of 2-oxo-*N*-(pyridin-4-yl)-2*H*-chromene-3-carboxamide

M. Sunithakumari,[a] M. Harish Kumar,[a] H. C. Devarajegowda,[a] M. U. Gagan,[b] V. Dwarakanath[b] and B. S. Palakshamurthy[c]*

[a]Department of Physics, Yuvaraja's College, University of Mysore, Mysore-570005, Karnataka, India, [b]Department of Biotechnology, U.C.S, Tumkur University, Tumkur, Karnataka-572103, India, and [c]Department of PG Studies and Research in Physics, Albert Einstein Block, UCS, Tumkur University, Tumkur, Karnataka-572103, India. *Correspondence e-mail: palaksha.bspm@gmail.com

Received 7 April 2026
Accepted 10 April 2026

Edited by L. Van Meervelt, Katholieke Universiteit Leuven, Belgium

Keywords: crystal structure; Hirshfeld surface; two-dimensional fingerprint; 2*H*-chromene-3-carboxamide.

CCDC reference: 2545176

Supporting information: this article has supporting information at journals.iucr.org/e

In the title compound, $C_{15}H_{10}N_2O_3$, the dihedral angle between the heterocyclic 2*H*-chromene and the pyridine moieties is 2.09 (9)°. The molecule exhibits an almost planar conformation (r.m.s. deviation = 0.048 Å). The torsion angle associated with the amide linkage between the 2*H*-chromene and pyridine moieties is −179.17 (18)° and found to be a*nti*-periplanar. In the crystal, C—H···O hydrogen bonds form two sets of inversion dimers, generating $R_2^2(14)$ and $R_2^2(16)$ synthons that propagate along the [010] direction. The molecular packing in the crystal is further consolidated by C═O···π interactions and π–π stacking with centroid–centroid separations of 3.732 (2), 3.815 (2) and 3.947 (2) Å. The two-dimensional fingerprint plots indicate that the major contributions to the crystal packing arise from H···O/O···H (19.5%), H···C/C···H (14.1%), H···N/N···H (8.0%) and O···C/C···O (5.0%) interactions.

1. Chemical context

The 2-oxo-2*H*-chromene (coumarin) scaffold is of considerable interest due to its diverse biological and physicochemical properties. Coumarin derivatives, both natural and synthetic, exhibit a broad range of pharmacological activities, including antioxidant, anti-inflammatory and anticoagulant effects (Annunziata *et al.*, 2020; Ivanov *et al.*, 2025). They have also been reported to show significant anticancer activity through inhibition of cell proliferation and modulation of signalling pathways (Emami & Dadashpour, 2015), as well as antimicrobial activity against pathogens such as *Staphylococcus aureus* and *Escherichia coli* (Tang *et al.*, 2025; Baaiu *et al.*, 2025). In addition to pharmaceutical relevance, coumarin derivatives find applications in other fields owing to their characteristic odour, fluorescence properties and agrochemical activity (Anywar & Muhumuza, 2024). In particular, chromene-3-carboxamide derivatives have attracted attention due to their cytotoxic activity and their ability to inhibit cancer-related enzymes such as carbonic anhydrase IX (Supuran *et al.*, 2017). These compounds also exhibit antibacterial activity against both Gram-positive and Gram-negative bacteria (Khan *et al.*, 2020).

Furthermore, the presence of amide and heterocyclic donor groups, such as pyridin-4-yl moieties, enhances their ability to coordinate with metal ions, making them useful in coordination chemistry and crystal engineering (El-Sayed *et al.*, 2023; Kaur *et al.*, 2015). Such coordination behaviour facilitates the formation of supramolecular assemblies and functional materials. On the basis of these considerations, coumarin–

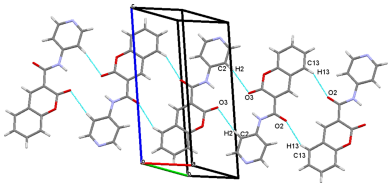

pyridine hybrid systems are of particular interest, and we report herein the synthesis and crystal structure of a new derivative.

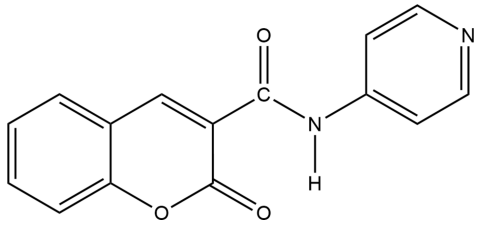

2. Structural commentary

In the title compound (Fig. 1), the fused 2*H*-chromene ring system (C8–C11/O1/C12–C16) and the pyridine ring (C1–C3/N2/C5/C6) are nearly coplanar, forming a dihedral angle of 2.09 (9)°, with an r.m.s. deviation of 0.048 Å, indicating an essentially planar conformation. The amide linkage between the 2*H*-chromene and pyridine moieties adopts an anti-periplanar conformation, as evidenced by the C8—C7(═O2)—N1—C1 torsion angle of −179.17 (18)°. Bond lengths and angles are within normal ranges. Intramolecular N1—H1···O3, C6—H6···O2 and C9—H9···O2 hydrogen bonds are observed (see Table 1 for details), contributing to the stabilization of the molecular conformation.

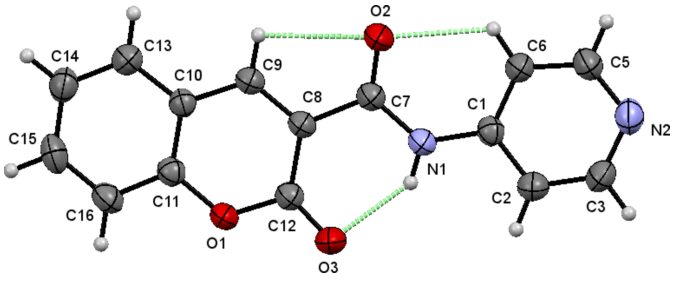

Figure 1
The title compound with the atom-numbering scheme and 50% probability ellipsoids.

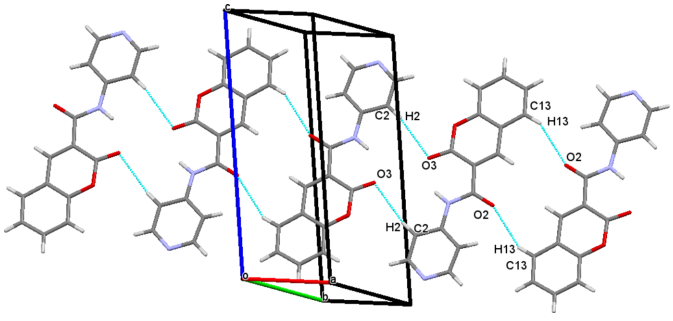

Figure 2
The packing of the title compound. Intermolecular C—H···O hydrogen bonds are shown as blue dashed lines.

Table 1
Hydrogen-bond geometry (Å, °).

D—H···*A*	*D*—H	H···*A*	*D*···*A*	*D*—H···*A*
N1—H1···O3	0.86	1.97	2.698 (2)	141
C6—H6···O2	0.93	2.29	2.869 (3)	120
C9—H9···O2	0.93	2.44	2.758 (3)	100
C2—H2···O3^{i}	0.93	2.58	3.480 (3)	162
C13—H13···O2^{ii}	0.93	2.59	3.422 (3)	149

Symmetry codes: (i) $-x+2, -y+2, -z+1$; (ii) $-x, -y+1, -z+1$.

3. Supramolecular features

In the crystal, the molecules are linked via C—H···O hydrogen bonds, giving rise to centrosymmetric inversion dimers (Table 1). On one side of the molecule, C2—H2···O3 interactions generate $R_2^2(16)$ ring motifs, while on the opposite side, C13—H13···O2 hydrogen bonds form $R_2^2(14)$ ring motifs. These discrete supramolecular synthons propagate along the [010] direction (Fig. 2). The crystal packing is further consolidated by C═O···π interactions involving the carbonyl group C7═O2 and the π-system of the 2*H*-chromene ring [Fig. 3; O2···*Cg*1($1-x, 1-y, 1-z$) = 3.279 (2) Å, *Cg*1 is the centroid of the O1/C8–C12 ring]. In addition, significant π–π stacking interactions are observed between adjacent aromatic systems (Fig. 4). The centroid–centroid separations are *Cg*1···*Cg*2($1-x, -y, 1-z$) = 3.815 (2) Å, *Cg*2···*Cg*3($1-x, 1-y, 1-z$) = 3.732 (2) Å and *Cg*2···*Cg*3($1-x, 2-y, 1-z$)

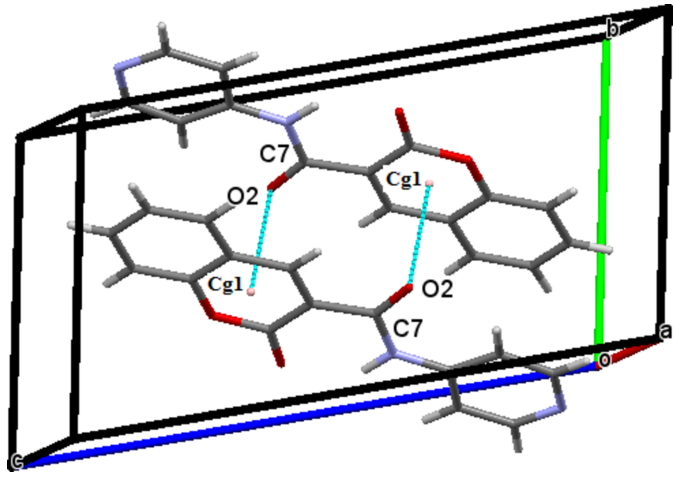

Figure 3
Partial crystal packing of the title compound showing the C—O···π interactions as blue dashed lines.

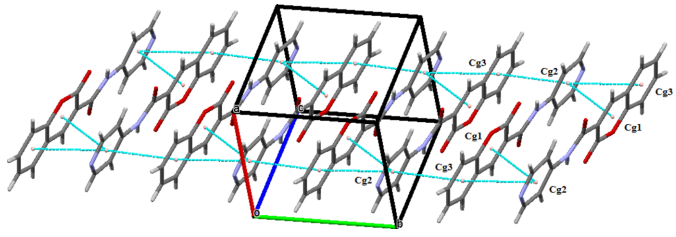

Figure 4
Crystal packing of the title compound showing the π–π interactions as blue dashed lines.

= 3.947 (2) Å, where *Cg*2 and *Cg*3 are the centroids of the pyridine (N2/C1–C3/C5–C6) and 2*H*-chromene benzene (C10/C11/C13–C16) rings, respectively. These non-covalent interactions collectively contribute to the cohesion of the three-dimensional crystal architecture.

4. Database survey

A search of the Cambridge Structural Database (CSD, version 5.43, 2025 update; Groom *et al.*, 2016) for structures containing the 2-oxo-2*H*-chromene-3-carboxamide moiety yielded more than 30 hits. Among these, closely related structures include 7-(diethylamino)-*N*-(4-nitrophenyl)-2-oxo-2*H*-chromene-3-carboxamide (refcode DISYIP; Maldonado-Domínguez *et al.*, 2014), 7-(diethylamino)-*N*-(4-fluorophenyl)-2-oxo-2*H*-chromene-3-carboxamide (DISXUA; Maldonado-Domínguez *et al.*, 2014), and 7-(diethylamino)-*N*-(3-methyl-1,3-benzothiazol-2(3*H*)-ylidene)-2-oxo-2*H*-chromene-3-carboxamide (DUBHOZ; Wang *et al.*, 2015), which exhibit dihedral angles of 0.28, 0.79 and 2.85°, respectively, indicating a strong tendency toward planarity in this class of compounds similar to the title molecule.

The torsional angle associated with the amide linkage in representative examples *N*-(3-(imidazo[1,2-*a*]pyridin-2-yl) phenyl)-8-methoxy-2-oxo-2*H*-chromene-3-carboxamide (BONKAS; Julien *et al.*, 2014), 7-(diethylamino)-*N*-(4-fluorophenyl)-2-oxo-2*H*-chromene-3-carboxamide, *N*-(4-cyanophenyl)-7-(diethylamino)-2-oxo-2*H*-chromene-3-carboxamide and 7-(diethylamino)-*N*-(4-nitrophenyl)-2-oxo-2*H*-chromene-3-carboxamide (DISXUA, DISYEL and DISYIP, respectively; Maldonado-Domínguez *et al.*, 2014) are 179.96, 177.26, −179.17 and −177.43°, respectively, reflecting an anti-periplanar conformation. In the representative examples 7-(diethylamino)-*N*-(3-methyl-1,3-benzothiazol-2(3*H*)-ylidene)-2-oxo-2*H*-chromene-3-carboxamide (DUBHOZ; Wang *et al.*, 2015) and 6-methoxy-*N*-(3-methylphenyl)-2-oxo-2*H*-chromene-3-carboxamide (ECEBIA; Gomes *et al.*, 2016) the torsion angles are −177.73 and −179.06°, respectively, reflecting the same anti-periplanar conformation as comparable to the title molecule.

5. Hirshfeld surface analysis

A Hirshfeld surface analysis of the title compound was carried out using *CrystalExplorer* (Spackman *et al.*, 2021) to investigate and visualize the intermolecular interactions governing the crystal packing. The Hirshfeld surface mapped over d_{norm} together with two neighbouring molecules is shown in Fig. 5,

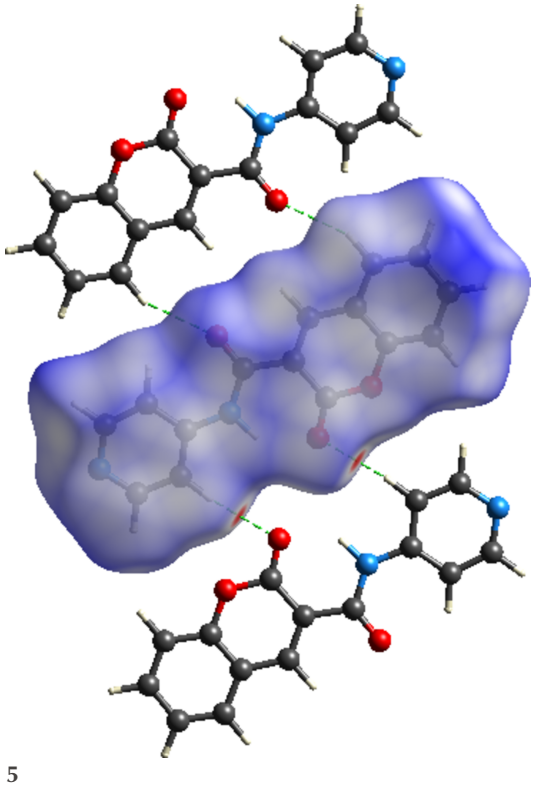

Figure 5
View of the three-dimensional Hirshfeld surface mapped over d_{norm} and the C—H···O interactions forming $R_2^2(16)$ and $R_2^2(14)$ ring motifs with neighboring molecules

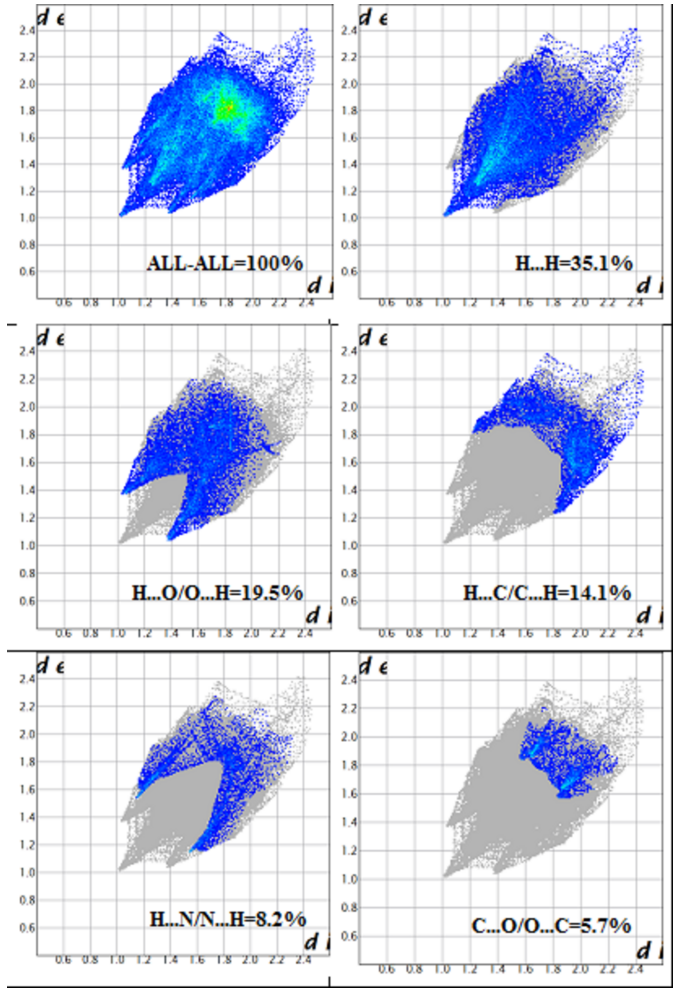

Figure 6
The two-dimensional fingerprint plots showing all (100%), H···H (31.5%), H···O/O···H (19.5%), H···C/C···H (14.1%), H···N/N···H (8.0%), and O···C/C···O (5.0%) contacts.

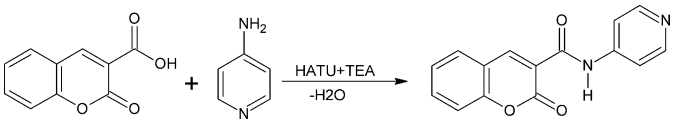

Figure 7
Reaction scheme for the synthesis of the title compound.

On one side of the molecule, the oxygen atom of the amide linkage takes part in C2—H2···O3 interactions generating $R_2^2(16)$ ring motifs, while on the opposite side, the oxygen of the 2-oxo-2*H*-chromene moiety takes part in C13—H13···O2 hydrogen bonds forming $R_2^2(14)$ ring motifs, where red spots correspond to regions of these close intermolecular contacts. The two-dimensional fingerprint plots provide a quantitative description of the various intermolecular interactions. The most significant contributions arise from H···H contacts (35.1%), followed by H···O/O···H (19.5%), H···C/C···H (14.1%), H···N/N···H (8.2%) and O···C/C···O (5.7%) interactions (Fig. 6). These results indicate that van der Waals interactions (H···H) dominate the crystal packing, while directional hydrogen-bonding and heteroatom contacts make notable secondary contributions.

6. Synthesis and crystallization

A mixture of 2-oxo-2*H*-chromene-3-carboxylic acid (1.00 mmol), 4-aminopyridine (2.00 mmol) and triethyl amine (TEA; 4.2 mmol) in acetonitrile (15 ml) was stirred at room temperature for 15 min. Then, 1-[bis(dimethylamino)methylene]-1*H*-1,2,3-triazolo[4,5-*b*]pyridinium 3-oxide hexafluorophosphate (HATU; 5 mmol) was added in one portion, and the reaction was covered with a rubber septum. After 24 h, the acetonitrile was removed *in vacuo*, and the residue was dissolved in dichloromethane (25 ml). The organic layer was washed with water (25 ml) and separated; the aqueous layer was extracted with dichloromethane. The combined organic layers were washed with brine, dried over magnesium sulfate, and concentrated under reduced pressure. The crude residue was purified by 60–120 mesh silica gel column chromatography (1:4 ethyl acetate:hexane). The scheme for the reaction is presented in Fig. 7.

7. Refinement

Crystal data, data collection and structure refinement details are summarized in Table 2. All H atoms were positioned with idealized geometry (N—H = 0.83 Å, C—H = 0.93 Å) and refined using a riding model with U_{iso}(H) = 1.2U_{eq}(C/N).

Table 2
Experimental details.

Crystal data	
Chemical formula	$C_{15}H_{10}N_2O_3$
M_r	266.25
Crystal system, space group	Triclinic, $P\overline{1}$
Temperature (K)	299
a, b, c (Å)	5.731 (2), 7.668 (3), 13.911 (5)
α, β, γ (°)	103.199 (14), 93.059 (11), 94.332 (10)
V (Å^3)	591.8 (4)
Z	2
Radiation type	Mo $K\alpha$
μ (mm^{-1})	0.11
Crystal size (mm)	0.32 × 0.27 × 0.24
Data collection	
Diffractometer	Bruker SMART APEXII CCD
Absorption correction	Multi-scan (*SADABS*; Krause *et al.*, 2015)
T_{min}, T_{max}	0.964, 0.973
No. of measured, independent and observed [$I > 2\sigma(I)$] reflections	8155, 3181, 2263
R_{int}	0.034
(sin $\theta/\lambda)_{max}$ (Å^{-1})	0.697
Refinement	
$R[F^2 > 2\sigma(F^2)]$, $wR(F^2)$, S	0.071, 0.184, 1.02
No. of reflections	3181
No. of parameters	181
H-atom treatment	H-atom parameters constrained
$\Delta\rho_{max}$, $\Delta\rho_{min}$ (e Å^{-3})	0.35, −0.22

Computer programs: *APEX2* and *SAINT* (Bruker, 2017), *SHELXT2018/3* (Sheldrick, 2015*a*), *SHELXL2019/3* (Sheldrick, 2015*b*), *Mercury* (Macrae *et al.*, 2020) and *publCIF* (Westrip, 2010).

Acknowledgements

The authors thank the Solid State and Structural Chemistry Unit (SSCU), Indian Institute of Science (IISc) and iSTEM facilities for their help with the single-crystal data collection. MSK thanks the BSPM lab, Centre of Innovative Science, Engineering and Education (CISEE) for extending their help in carrying out experiments and use of software facilities to complete the research work at University College of Science (UCS), Tumkur University Tumkur.

References

Annunziata, F., Pinna, C., Dallavalle, S., Tamborini, L. & Pinto, A. (2020). *Int. J. Mol. Sci.* **21**, 4618.
Anywar, G. & Muhumuza, E. (2024). *Front. Pharmacol.* **14**, 1231006.
Baaiu, B. S., Saleh, N. M., Alshref Aldirsi, A. F. & Abdel-Aziem, A. (2025). *Future Med. Chem.* **17**, 9–18.
Bruker (2017). *APEX2* and *SAINT*. Bruker AXS Inc., Madison, Wisconsin, USA.
El-Sayed, A., Hassan, A. & Ahmed, M. (2023). *Inorg. Chem. Commun.* **152**, 110725.
Emami, S. & Dadashpour, S. (2015). *Eur. J. Med. Chem.* **102**, 611–630.
Gomes, L. R., Low, J. N., Fonseca, A., Matos, M. J. & Borges, F. (2016). *Acta Cryst.* E**72**, 926–932.
Groom, C. R., Bruno, I. J., Lightfoot, M. P. & Ward, S. C. (2016). *Acta Cryst.* B**72**, 171–179.
Ivanov, I., Manolov, S., Dimitrova, D. & Nedialkov, P. (2025). *Molbank* M1968.
Julien, O., Kampmann, M., Bassik, M. C., Zorn, J. A., Venditto, V. J., Shimbo, K., Agard, N. J., Shimada, K., Rheingold, A. L., Stockwell, B. R., Weissman, J. S. & Wells, J. A. (2014). *Nat. Chem. Biol.* **10**, 969–976.
Kaur, M., Kohli, S., Sandhu, S., Bansal, Y. & Bansal, G. (2015). *Anti-Cancer Agents Med. Chem.* **15**, 1032–1048.
Khan, M., Ahmad, S. & Ali, M. (2020). *Hellyon* **5**, e02605.
Krause, L., Herbst-Irmer, R., Sheldrick, G. M. & Stalke, D. (2015). *J. Appl. Cryst.* **48**, 3–10.

Macrae, C. F., Sovago, I., Cottrell, S. J., Galek, P. T. A., McCabe, P., Pidcock, E., Platings, M., Shields, G. P., Stevens, J. S., Towler, M. & Wood, P. A. (2020). *J. Appl. Cryst.* **53**, 226–235.

Maldonado-Domínguez, M., Arcos-Ramos, R., Romero, M., Flores-Pérez, B., Farfán, N., Santillan, R., Lacroix, P. G. & Malfant, I. (2014). *New J. Chem.* **38**, 260–268.

Sheldrick, G. M. (2015*a*). *Acta Cryst.* A**71**, 3–8.

Sheldrick, G. M. (2015*b*). *Acta Cryst.* C**71**, 3–8.

Spackman, P. R., Turner, M. J., McKinnon, J. J., Wolff, S. K., Grimwood, D. J., Jayatilaka, D. & Spackman, M. A. (2021). *J. Appl. Cryst.* **54**, 1006–1011.

Supuran, C. T. (2017). *Metabolites* **7**, 48.

Tang, Q., Zhang, H., Chandarajoti, K., Jiao, Z., Nie, L., Lv, S., Zuo, J., Zhou, W. & Han, X. (2025). *Med. Chem.* **16**, 1223–1234.

Wang, K., Liu, Z., Guan, R., Cao, D., Chen, H., Shan, Y., Wu, Q. & Xu, Y. (2015). *Spectrochim. Acta A Mol. Biomol. Spectrosc.* **144**, 235–242.

Westrip, S. P. (2010). *J. Appl. Cryst.* **43**, 920–925.

supporting information

Acta Cryst. (2026). E**82**, 516-520 [https://doi.org/10.1107/S2056989026003798]

Synthesis, crystal structure and Hirshfeld surface analysis of 2-oxo-*N*-(pyridin-4-yl)-2*H*-chromene-3-carboxamide

M. Sunithakumari, M. Harish Kumar, H. C. Devarajegowda, M. U. Gagan, V. Dwarakanath and B. S. Palakshamurthy

Computing details

2-Oxo-*N*-(pyridin-4-yl)-2*H*-chromene-3-carboxamide

Crystal data

$C_{15}H_{10}N_2O_3$
$M_r = 266.25$
Triclinic, $P\overline{1}$
Hall symbol: -P 1
$a = 5.731$ (2) Å
$b = 7.668$ (3) Å
$c = 13.911$ (5) Å
$\alpha = 103.199$ (14)°
$\beta = 93.059$ (11)°
$\gamma = 94.332$ (10)°
$V = 591.8$ (4) Å^3
$Z = 2$
$F(000) = 276$
$D_x = 1.494$ Mg m^{-3}
Melting point: 410 K
Mo $K\alpha$ radiation, $\lambda = 0.71073$ Å
Cell parameters from 2253 reflections
$\theta = 0.2$–$29.0°$
$\mu = 0.11$ mm^{-1}
$T = 299$ K
Prism, colourless
0.32 × 0.27 × 0.24 mm

Data collection

Bruker SMART APEXII CCD diffractometer
Radiation source: fine-focus sealed tube
Graphite monochromator
Detector resolution: 1.7 pixels mm^{-1}
φ and Ω scans
Absorption correction: multi-scan (SADABS; Krause *et al.*, 2015)
$T_{min} = 0.964$, $T_{max} = 0.973$
8155 measured reflections
3181 independent reflections
2263 reflections with $I > 2\sigma(I)$
$R_{int} = 0.034$
$\theta_{max} = 29.7°$, $\theta_{min} = 2.7°$
$h = -7 \rightarrow 7$
$k = -10 \rightarrow 8$
$l = -19 \rightarrow 19$

Refinement

Refinement on F^2
Least-squares matrix: full
$R[F^2 > 2\sigma(F^2)] = 0.071$
$wR(F^2) = 0.184$
$S = 1.02$
3181 reflections
181 parameters
0 restraints
0 constraints
Primary atom site location: structure-invariant direct methods
Secondary atom site location: difference Fourier map
Hydrogen site location: inferred from neighbouring sites
H-atom parameters constrained
$w = 1/[\sigma^2(F_o^2) + (0.0775P)^2 + 0.3022P]$ where $P = (F_o^2 + 2F_c^2)/3$
$(\Delta/\sigma)_{max} < 0.001$
$\Delta\rho_{max} = 0.35$ e Å^{-3}
$\Delta\rho_{min} = -0.22$ e Å^{-3}

Special details

Geometry. All esds (except the esd in the dihedral angle between two l.s. planes) are estimated using the full covariance matrix. The cell esds are taken into account individually in the estimation of esds in distances, angles and torsion angles; correlations between esds in cell parameters are only used when they are defined by crystal symmetry. An approximate (isotropic) treatment of cell esds is used for estimating esds involving l.s. planes.

Fractional atomic coordinates and isotropic or equivalent isotropic displacement parameters (Å²)

	x	*y*	*z*	U_{iso}*/U_{eq}
O1	0.6621 (2)	0.66045 (19)	0.30075 (10)	0.0408 (4)
N1	0.5999 (3)	0.8748 (2)	0.60639 (12)	0.0391 (4)
H1	0.709158	0.903908	0.571403	0.047*
C1	0.6267 (3)	0.9567 (2)	0.70744 (14)	0.0343 (4)
O2	0.2543 (3)	0.7009 (2)	0.59463 (11)	0.0530 (5)
C2	0.8347 (4)	1.0609 (3)	0.74418 (16)	0.0429 (5)
H2	0.951919	1.076508	0.702375	0.051*
O3	0.8239 (3)	0.8350 (2)	0.43803 (12)	0.0546 (5)
C3	0.8642 (4)	1.1408 (3)	0.84403 (17)	0.0489 (6)
H3	1.003647	1.211559	0.867377	0.059*
N2	0.7074 (4)	1.1241 (3)	0.90939 (14)	0.0500 (5)
C5	0.5084 (4)	1.0255 (3)	0.87212 (16)	0.0463 (5)
H5	0.394600	1.012612	0.915832	0.056*
C6	0.4575 (4)	0.9411 (3)	0.77383 (15)	0.0407 (5)
H6	0.313624	0.875356	0.752407	0.049*
C7	0.4221 (3)	0.7544 (3)	0.55616 (15)	0.0368 (4)
C8	0.4456 (3)	0.6886 (3)	0.44736 (14)	0.0339 (4)
C9	0.2666 (3)	0.5796 (3)	0.39258 (14)	0.0357 (4)
H9	0.133815	0.550586	0.423391	0.043*
C10	0.2754 (3)	0.5076 (3)	0.28884 (14)	0.0343 (4)
C11	0.4783 (3)	0.5494 (3)	0.24507 (14)	0.0354 (4)
C12	0.6545 (4)	0.7357 (3)	0.39968 (14)	0.0374 (4)
C13	0.0925 (4)	0.3980 (3)	0.22872 (16)	0.0430 (5)
H13	−0.045401	0.368823	0.256137	0.052*
C14	0.1153 (4)	0.3332 (3)	0.12939 (16)	0.0471 (5)
H14	−0.007513	0.261687	0.089546	0.056*
C15	0.3218 (4)	0.3747 (3)	0.08887 (16)	0.0486 (6)
H15	0.337020	0.328822	0.021821	0.058*
C16	0.5058 (4)	0.4830 (3)	0.14592 (15)	0.0443 (5)
H16	0.644142	0.510211	0.118265	0.053*

Atomic displacement parameters (Å²)

	U^{11}	U^{22}	U^{33}	U^{12}	U^{13}	U^{23}
O1	0.0374 (8)	0.0506 (9)	0.0319 (7)	−0.0050 (6)	0.0080 (6)	0.0060 (6)
N1	0.0397 (9)	0.0443 (10)	0.0312 (8)	−0.0038 (7)	0.0077 (7)	0.0060 (7)
C1	0.0399 (10)	0.0314 (9)	0.0316 (9)	0.0028 (8)	0.0029 (8)	0.0071 (7)
O2	0.0484 (9)	0.0697 (11)	0.0352 (8)	−0.0153 (8)	0.0113 (7)	0.0051 (7)
C2	0.0406 (11)	0.0458 (12)	0.0414 (11)	−0.0025 (9)	0.0062 (9)	0.0099 (9)

O3	0.0417 (9)	0.0716 (11)	0.0425 (9)	−0.0166 (8)	0.0091 (7)	0.0029 (8)
C3	0.0470 (12)	0.0492 (13)	0.0440 (12)	−0.0108 (10)	−0.0022 (10)	0.0034 (10)
N2	0.0584 (12)	0.0505 (11)	0.0364 (10)	−0.0014 (9)	0.0012 (8)	0.0026 (8)
C5	0.0511 (13)	0.0494 (12)	0.0361 (11)	0.0007 (10)	0.0094 (9)	0.0051 (9)
C6	0.0395 (11)	0.0416 (11)	0.0371 (11)	−0.0039 (8)	0.0042 (8)	0.0035 (8)
C7	0.0386 (10)	0.0386 (10)	0.0326 (10)	0.0012 (8)	0.0043 (8)	0.0073 (8)
C8	0.0344 (10)	0.0371 (10)	0.0306 (9)	0.0011 (8)	0.0053 (7)	0.0088 (7)
C9	0.0353 (10)	0.0386 (10)	0.0337 (10)	0.0011 (8)	0.0059 (8)	0.0093 (8)
C10	0.0372 (10)	0.0338 (10)	0.0313 (10)	0.0033 (8)	0.0031 (8)	0.0065 (7)
C11	0.0384 (10)	0.0342 (10)	0.0339 (10)	0.0025 (8)	0.0044 (8)	0.0084 (8)
C12	0.0395 (10)	0.0386 (10)	0.0334 (10)	0.0006 (8)	0.0056 (8)	0.0073 (8)
C13	0.0411 (11)	0.0443 (12)	0.0412 (12)	−0.0013 (9)	0.0039 (9)	0.0062 (9)
C14	0.0520 (13)	0.0454 (12)	0.0389 (11)	−0.0011 (10)	−0.0027 (10)	0.0028 (9)
C15	0.0678 (15)	0.0482 (13)	0.0284 (10)	0.0098 (11)	0.0049 (10)	0.0045 (9)
C16	0.0479 (12)	0.0509 (13)	0.0356 (11)	0.0037 (10)	0.0118 (9)	0.0116 (9)

Geometric parameters (Å, º)

O1—C12	1.370 (2)	C5—H5	0.9300
O1—C11	1.382 (2)	C6—H6	0.9300
N1—C7	1.366 (3)	C7—C8	1.499 (3)
N1—C1	1.398 (2)	C8—C9	1.352 (3)
N1—H1	0.8600	C8—C12	1.461 (3)
C1—C2	1.388 (3)	C9—C10	1.428 (3)
C1—C6	1.391 (3)	C9—H9	0.9300
O2—O2	0.000 (5)	C10—C11	1.391 (3)
O2—O2	0.000 (5)	C10—C13	1.399 (3)
O2—C7	1.215 (2)	C11—C16	1.379 (3)
C2—C3	1.380 (3)	C13—C14	1.374 (3)
C2—H2	0.9300	C13—H13	0.9300
O3—O3	0.000 (5)	C14—C15	1.384 (3)
O3—C12	1.206 (2)	C14—H14	0.9300
C3—N2	1.332 (3)	C15—C16	1.381 (3)
C3—H3	0.9300	C15—H15	0.9300
N2—C5	1.330 (3)	C16—H16	0.9300
C5—C6	1.378 (3)		
C12—O1—C11	122.70 (15)	C9—C8—C7	118.04 (17)
C7—N1—C1	128.19 (17)	C12—C8—C7	122.45 (17)
C7—N1—H1	115.9	C8—C9—C10	121.95 (18)
C1—N1—H1	115.9	C8—C9—H9	119.0
C2—C1—C6	117.69 (18)	C10—C9—H9	119.0
C2—C1—N1	118.11 (18)	C11—C10—C13	118.14 (18)
C6—C1—N1	124.20 (18)	C11—C10—C9	117.87 (18)
C3—C2—C1	118.6 (2)	C13—C10—C9	123.99 (18)
C3—C2—H2	120.7	C16—C11—O1	117.38 (17)
C1—C2—H2	120.7	C16—C11—C10	122.19 (19)
N2—C3—C2	124.8 (2)	O1—C11—C10	120.43 (17)

N2—C3—H3	117.6	O3—C12—O1	115.52 (17)
C2—C3—H3	117.6	O3—C12—O1	115.52 (17)
C5—N2—C3	115.42 (19)	O3—C12—C8	127.00 (19)
N2—C5—C6	125.1 (2)	O3—C12—C8	127.00 (19)
N2—C5—H5	117.4	O1—C12—C8	117.48 (17)
C6—C5—H5	117.4	C14—C13—C10	120.4 (2)
C5—C6—C1	118.3 (2)	C14—C13—H13	119.8
C5—C6—H6	120.8	C10—C13—H13	119.8
C1—C6—H6	120.8	C13—C14—C15	119.8 (2)
O2—C7—N1	123.95 (19)	C13—C14—H14	120.1
O2—C7—N1	123.95 (19)	C15—C14—H14	120.1
O2—C7—N1	123.95 (19)	C16—C15—C14	121.4 (2)
O2—C7—C8	120.60 (18)	C16—C15—H15	119.3
O2—C7—C8	120.60 (18)	C14—C15—H15	119.3
O2—C7—C8	120.60 (18)	C11—C16—C15	118.08 (19)
N1—C7—C8	115.45 (16)	C11—C16—H16	121.0
C9—C8—C12	119.50 (18)	C15—C16—H16	121.0
C7—N1—C1—C2	173.33 (19)	C8—C9—C10—C11	1.6 (3)
C7—N1—C1—C6	−6.9 (3)	C8—C9—C10—C13	−178.3 (2)
C6—C1—C2—C3	0.9 (3)	C12—O1—C11—C16	179.46 (18)
N1—C1—C2—C3	−179.3 (2)	C12—O1—C11—C10	−0.7 (3)
C1—C2—C3—N2	0.8 (4)	C13—C10—C11—C16	−1.7 (3)
C2—C3—N2—C5	−1.7 (4)	C9—C10—C11—C16	178.44 (19)
C3—N2—C5—C6	0.8 (4)	C13—C10—C11—O1	178.54 (18)
N2—C5—C6—C1	0.9 (4)	C9—C10—C11—O1	−1.4 (3)
C2—C1—C6—C5	−1.7 (3)	C11—O1—C12—O3	−177.37 (18)
N1—C1—C6—C5	178.55 (19)	C11—O1—C12—O3	−177.37 (18)
C1—N1—C7—O2	0.6 (3)	C11—O1—C12—C8	2.5 (3)
C1—N1—C7—O2	0.6 (3)	C9—C8—C12—O3	177.6 (2)
C1—N1—C7—O2	0.6 (3)	C7—C8—C12—O3	−3.4 (3)
C1—N1—C7—C8	−179.17 (18)	C9—C8—C12—O3	177.6 (2)
O2—C7—C8—C9	5.0 (3)	C7—C8—C12—O3	−3.4 (3)
O2—C7—C8—C9	5.0 (3)	C9—C8—C12—O1	−2.3 (3)
O2—C7—C8—C9	5.0 (3)	C7—C8—C12—O1	176.68 (17)
N1—C7—C8—C9	−175.21 (18)	C11—C10—C13—C14	0.5 (3)
O2—C7—C8—C12	−174.0 (2)	C9—C10—C13—C14	−179.6 (2)
O2—C7—C8—C12	−174.0 (2)	C10—C13—C14—C15	0.8 (3)
O2—C7—C8—C12	−174.0 (2)	C13—C14—C15—C16	−1.0 (4)
N1—C7—C8—C12	5.8 (3)	O1—C11—C16—C15	−178.72 (18)
C12—C8—C9—C10	0.3 (3)	C10—C11—C16—C15	1.5 (3)
C7—C8—C9—C10	−178.74 (17)	C14—C15—C16—C11	−0.1 (3)

Hydrogen-bond geometry (Å, º)

D—H···*A*	*D*—H	H···*A*	*D*···*A*	*D*—H···*A*
N1—H1···O3	0.86	1.97	2.698 (2)	141
C6—H6···O2	0.93	2.29	2.869 (3)	120

C9—H9···O2	0.93	2.44	2.758 (3)	100
C2—H2···O3^{i}	0.93	2.58	3.480 (3)	162
C13—H13···O2^{ii}	0.93	2.59	3.422 (3)	149

Symmetry codes: (i) −*x*+2, −*y*+2, −*z*+1; (ii) −*x*, −*y*+1, −*z*+1.